HEPATOLOGY

HEPATOLOGY, VOL. 72, NO. 3, 2020

Acyl-Coenzyme A Thioesterase 9 Traffics Mitochondrial Short-Chain Fatty Acids Toward *De Novo* Lipogenesis and Glucose Production in the Liver

Sandra Steensels,[1] Jixuan Qiao,[1] Yanzhen Zhang,[2] Kristal M. Maner-Smith,[3] Nourhan Kika,[1] Corey D. Holman,[1] Kathleen E. Corey,[4] W. Clay Bracken,[5] Eric A. Ortlund,[3] and Baran A. Ersoy [1]

SEE EDITORIAL ON PAGE 797

BACKGROUND AND AIMS: Obesity-induced pathogenesis of nonalcoholic fatty liver disease (NAFLD) and nonalcoholic steatohepatitis (NASH) is associated with increased *de novo* lipogenesis (DNL) and hepatic glucose production (HGP) that is due to excess fatty acids. Acyl-coenzyme A (CoA) thioesterase (Acot) family members control the cellular utilization of fatty acids by hydrolyzing (deactivating) acyl-CoA into nonesterified fatty acids and CoASH.

APPROACH AND RESULTS: Using *Caenorhabditis elegans*, we identified Acot9 as the strongest regulator of lipid accumulation within the Acot family. Indicative of a maladaptive function, hepatic Acot9 expression was higher in patients with obesity who had NAFLD and NASH compared with healthy controls with obesity. In the setting of excessive nutrition, global ablation of Acot9 protected mice against increases in weight gain, HGP, steatosis, and steatohepatitis. Supportive of a hepatic function, the liver-specific deletion of Acot9 inhibited HGP and steatosis in mice without affecting diet-induced weight gain. By contrast, the rescue of Acot9 expression only in the livers of Acot9 knockout mice was sufficient to promote HGP and steatosis. Mechanistically, hepatic Acot9 localized to the inner mitochondrial membrane, where it deactivated short-chain but not long-chain fatty acyl-CoA. This unique localization and activity of Acot9 directed acetyl-CoA away from protein lysine acetylation and toward the citric acid (TCA) cycle. Acot9-mediated exacerbation of triglyceride and glucose biosynthesis was attributable at least in part to increased TCA cycle activity, which provided substrates for HGP and DNL. β-oxidation and ketone body production, which depend on long-chain fatty acyl-CoA, were not regulated by Acot9.

CONCLUSIONS: Taken together, our findings indicate that Acot9 channels hepatic acyl-CoAs toward increased HGP and DNL under the pathophysiology of obesity. Therefore, Acot9 represents a target for the management of NAFLD. (Hepatology 2020;72:857-872).

Nonalcoholic fatty liver disease (NAFLD) has emerged as a global epidemic, with a worldwide prevalence over 25%.[1] Hallmarked by hepatic steatosis and increased hepatic glucose production (HGP),[2] the pathogenesis of NAFLD has been mechanistically linked to alterations in fatty acid utilization.[3]

Hepatic fatty acids, which originate from *de novo* lipogenesis (DNL) or uptake of circulatory

Abbreviations: ACC, acetyl-coenzyme A carboxylase; Acot, acyl-coenzyme A thioesterase; AcK, lysine acetylation; Ad-flp, adenovirus expressing flp recombinase; CoA, coenzyme A; Cyt C, cytochrome C; DNL, de novo *lipogenesis; EE, energy expenditure; ER, endoplasmic reticulum; Flp, flippase; FPC, fructose, palmitate, and cholesterol; FRT, flippase recognition target; HFD, high-fat diet; HGP, hepatic glucose production; Hsp90, heat shock protein 90; IM, inner membrane; IMS, intermembrane space; NAFLD, nonalcoholic fatty liver disease; NEFA, nonesterified fatty acids; NASH, nonalcoholic steatohepatitis; OM, outer membrane; PTT, pyruvate tolerance test; SCFA, short-chain fatty acids; Tbg, human thyroxine binding globulin; TCA, citric acid ; TG, triglyceride; VCO_2, carbon dioxide production; VLDL, very low density lipoprotein; WT, wild type.*

Received September 23, 2019; accepted May 16, 2020.

Additional Supporting Information may be found at onlinelibrary.wiley.com/doi/10.1002/hep.31409/suppinfo.

Supported by National Institute of Diabetes and Digestive and Kidney Diseases (R03 DK117247 to B.A.E. and K23 DK099422 to K.E.C.); National Institutes of Health Shared Instrumentation Grant (S10 OD016320 to W.C.B.); Weill Cornell Department of Medicine (Startup funds and Seed Grant for Innovative Research to B.A.E); the Georgia Clinical & Translational Science Alliance of the National Institutes of Health (UL1TR002378 to E.A.O.); the American Liver Foundation (Alexander M. White, III Memorial Postdoctoral Research Fellowship Award to S.S.); a Belgian American Educational Foundation (Postdoctoral Fellowship to S.S.); the Weill Cornell Metabolic Phenotyping Core; and the Emory Integrated Lipidomics Core, which is subsidized by the Emory University School of Medicine.

chylomicrons and nonesterified fatty acids (NEFA), are immediately activated within the hepatocyte to form acyl-coenzyme A (CoA) molecules. Hepatic metabolic processes that require acyl-CoA, such as β-oxidation, lipogenesis, complex lipid synthesis, or very low density lipoprotein (VLDL) secretion, occur in distinct subcellular compartments. Trafficking of fatty acids toward utilization in specific metabolic pathways depends on their subcellular bioavailability, which is controlled by compartmentalized deactivation (hydrolysis of CoA) by acyl-CoA thioesterases (Acot), followed by reactivation (esterification to CoA) by acyl-CoA synthetases (Acs).[4-6] For instance, Acs long-chain family member 1 and Acot13 increase the bioavailability of acyl-CoA for either β-oxidation in the mitochondria or glycerolipid biosynthesis in the endoplasmic reticulum (ER) in response to metabolic demands of the hepatocyte.[5-9] Whereas the perpetual actions of 26 Acs and 15 Acot family members maintain lipid homeostasis in health, we have shown that obesity-induced activation of Acots, in response to excess fatty acids, can instead traffic excess acyl-CoA toward lipotoxic pathways, such as increased accumulation of saturated phospholipids and VLDL secretion.[8,9]

In the current study, we demonstrate that hepatic Acot9 (synonym: mt-Act48, mitochondrial Acot of 48 kDa) expression increases in the setting of NAFLD in mice and patients with obesity. Despite exhibiting broad substrate specificity *in vitro*, Acot9 is a mitochondrial protein that is enriched in many oxidative tissues and represents the main short-chain Acot within the mitochondria.[10] However, the biological function of Acot9 in health and disease is unknown. To gain insights, we generated mice lacking Acot9 expression ($Acot9^{-/-}$), which revealed key regulatory contributions to diet-induced adiposity, HGP, and hepatic steatosis. Mechanistic studies indicated that diet-induced activation of Acot9 does not affect hepatic β-oxidation but sequesters short-chain acyl-CoAs, such as acetyl-CoA, butyryl-CoA, and propionyl-CoA, within the mitochondrial matrix by deactivating them at the inner mitochondrial membrane. This in turn increases the substrate bioavailability for the citric acid (TCA) cycle and the biosynthesis of substrates for DNL and HGP. Overall, our results unveil a maladaptive mechanism that promotes the pathogenesis of NAFLD by fueling the TCA cycle in the setting of excessive nutrition.

Materials and Methods

Please visit the Supporting Information for a detailed description of experimental procedures.

ANIMALS AND DIETS

Animals were kept on C57BL/6J background for all crosses. $Acot9^{+/+}$, $Acot9^{Tg}$ and $Acot9^{-/-}$ mice were generated in our laboratory. All animals were maintained in barrier animal facilities at Weill Cornell Medical College per Institutional Animal Care and Use Committee guidelines and under approved animal

View this article online at wileyonlinelibrary.com.
DOI 10.1002/hep.31409

Potential conflict of interest: Dr. Corey consults for and received grants from Bristol-Myers Squibb. She consults for Novo Nordisk and received grants from Boehringer Ingelheim.

ARTICLE INFORMATION:

From the [1]Joan & Sanford I. Weill Department of Medicine, Weill Cornell Medical College, New York, NY; [2]Department of Gastroenterology, First Affiliated Hospital of Zhengzhou University, Zhengzhou, China; [3]Emory Integrated Lipidomics Core, Emory University, Atlanta, GA; [4]Gastrointestinal Unit, Massachusetts General Hospital, Boston, MA; [5]Department of Biochemistry, Weill Cornell Medical College, New York, NY.

ADDRESS CORRESPONDENCE AND REPRINT REQUESTS TO:

Baran A. Ersoy, Ph.D.
Joan & Sanford I. Weill Department of Medicine
Weill Cornell Medical College
413 E 69th St., Belfer Research Building, Room 628
New York, NY, 10021
E-mail: bersoy@med.cornell.edu
Tel.: +1-646-962-7675

protocols. Mice were housed in a 12-hour light/dark cycle barrier facility with free access to drinking water and were fed a standard chow diet (PicoLab Rodent Diet 20, 5053; LabDiets, St. Louis, MO). For diet-induced obesity, 4-week-old mice were fed HFD (60% kcal from fat; D12492; Research Diets, New Brunswick, NJ) for 11 weeks. For the experiments in thermoneutral housing, 4-week-old mice

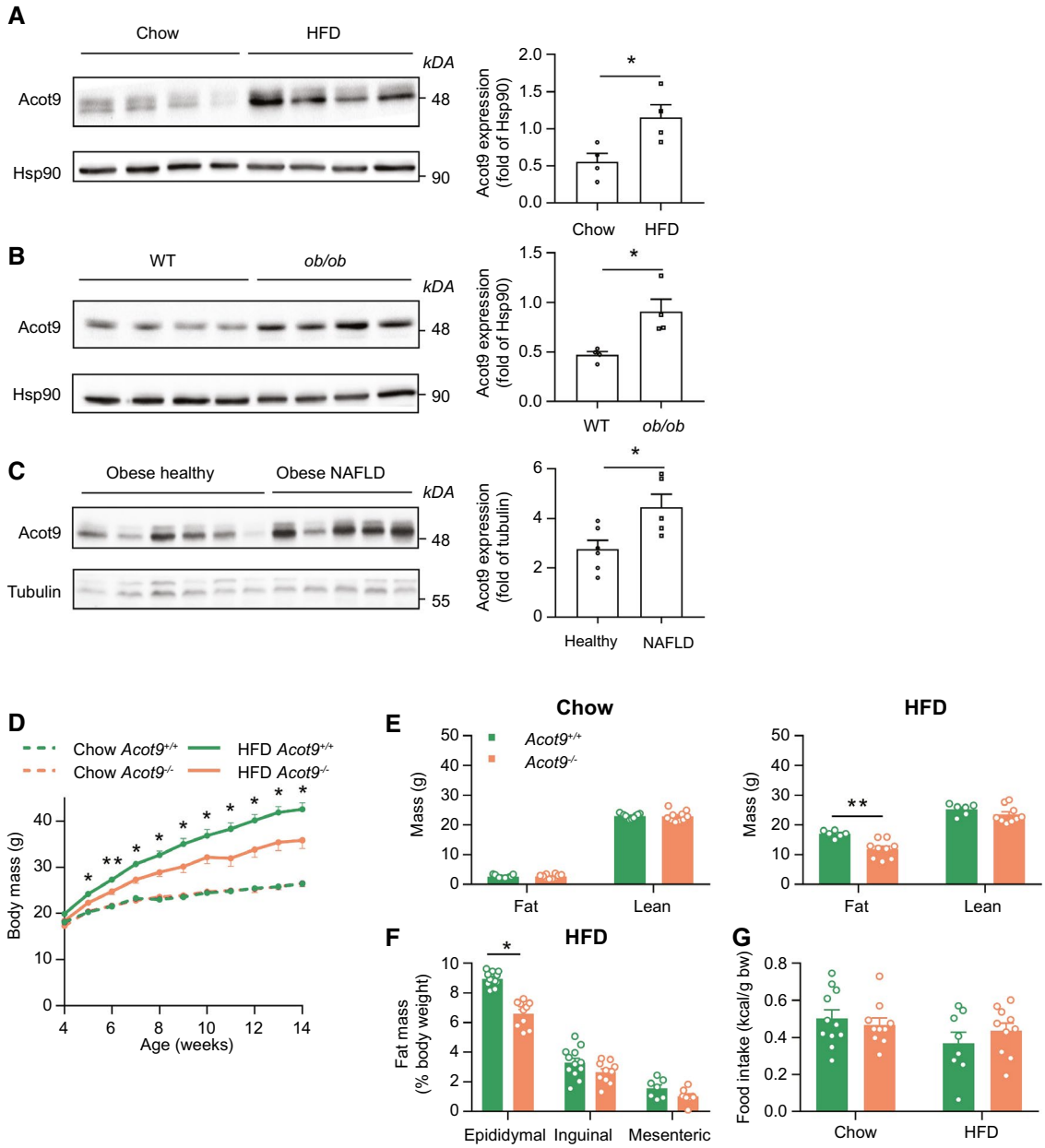

FIG. 1. Acot9 expression increases in the setting of obesity and liver disease and promotes body weight gain and adiposity. (A-C) Immunoblot analysis of Acot9 expression in the liver. (A) 4-week-old mice were fed chow or HFD (60% kcal) for 12 weeks. (B) 10-week-old chow-fed WT and *ob/ob* mice. (C) Healthy and steatotic liver biopsies from obese humans (body mass index >36). Inset barplots represent densitometry analyses normalized to heat shock protein 90 (Hsp90) or tubulin as loading control. (D-G) 4-week-old mice were weaned to chow ($Acot9^{+/+}$, n = 11; $Acot9^{-/-}$, n = 11) or HFD ($Acot9^{+/+}$, n = 11; $Acot9^{-/-}$, n = 11) for 11 weeks. (D) Body weight curve. (E) Fat mass and lean mass were measured using EchoMRI. (F) Epididymal, inguinal and mesenteric fat depots were dissected, and weights were normalized to body weight. (G) Food consumption was measured for 24 hours between 10 and 11 weeks of age. Error bars represent SEM. $^{*}P < 0.05$; $^{**}P < 0.01$ versus control or $Acot9^{+/+}$.

were housed in temperature-controlled environmental enclosures (DB034 Laboratory Incubator, Darwin Chambers, St. Louis, MO) at 30˚C in a 12-hour light/dark cycle system with free access to drinking water and were fed HFD for 8 weeks. Before collection of blood and tissues, mice were fasted for 6 hours during light cycle with free access to water unless stated otherwise. Blood was collected by cardiac puncture, and tissue samples were used immediately or snap-frozen in liquid nitrogen and stored at -80˚C. Plasma glucose concentrations were determined using a GE100 Blood Glucose Monitoring System (GE, Ontario, CA). Blood was centrifuged (16,000*g* for 15 minutes at 4˚C) and plasma was collected and stored at -80˚C. TG, phospholipid, NEFA, total cholesterol E, and free cholesterol concentrations were measured enzymatically using reagent kits (Wako Diagnostics, Mountain View, CA) according to the manufacturer's instructions as described.[31] Plasma insulin concentrations were determined using the Ultra Sensitive Mouse Insulin ELISA Kit (Crystal Chem, Elk Groove Village, IL).

PRIMARY HEPATOCYTE ISOLATION

Hepatocytes were isolated from 12-week-old chow-fed mice and cultured as described.[7] Isolated hepatocytes were plated at the density of 5×10^5 cells per well on either 6-well or 35 mm Primaria plates (Corning, Tewksbury, MA) in Williams' E medium (Invitrogen) containing 10% fetal bovine serum, penicillin (100 U/mL), and streptomycin (100 μg/mL). Cells were allowed to attach overnight before experimental procedures unless noted otherwise.

HUMAN LIVER SAMPLES

Liver biopsy specimens from participants undergoing weight loss operations were obtained from the NAFLD Biorepository of the Massachusetts General Hospital (Boston, MA). Participants underwent fasting blood samples within 8 months of their liver biopsy, and the presence of comorbid diseases was assessed by their treating physician. Liver biopsies were reviewed by a single blinded hepatopathologist and assigned a score for grade of steatosis, hepatocyte ballooning, and lobular inflammation.[9] Steatosis was defined as the presence of more than 5% fat without evidence of hepatocyte ballooning, lobular inflammation, or fibrosis. Patients gave informed consent at the time of recruitment, and studies were approved by the Partners Health Care Human Research Committee. Patient characteristics are listed in Supporting Table S2.

STATISTICAL ANALYSES

Data are reported as means ± SEM. Differences between groups were assessed using a two-tailed unpaired Student *t* test using a Bonferroni correction for multiple testing (Prism 7; GraphPad Software Inc., La Jolla, CA). Pathway analysis for metabolomics was performed using MetaboAnalyst software. Metabolites were included with $P < 0.1$. For studies at thermoneutrality, liver TG were adjusted to body fat percentage by analysis of covariance. *P* values of <0.05 were considered statistically significant.

Results

HEPATIC Acot9 EXPRESSION INCREASES IN THE SETTING OF OBESITY AND NAFLD

To determine which Acot family member has greater control over lipid accumulation, we monitored the role of Acot expression in *Caenorhabditis elegans*, which do not possess adipocytes but store their lipids in ectopic tissues.[12] RNA interference-mediated knockdown of Acot orthologues identified Acot9 (T22B7.7 and T07D3.9) as the strongest regulator of lipid accumulation (Supporting Fig. S1). To determine whether the activity of Acot9 was altered in the setting of metabolic liver disease, we monitored the expression of Acot9 in the livers of mice and humans with NAFLD. In mice, Acot9 expression increased by more than 2-fold following induction of NAFLD by either high-fat diet (HFD) or genetic ablation of leptin expression (*ob/ob*) (Fig. 1A,B). Suggestive of a maladaptive response, the livers of patients with obesity and NAFLD expressed 1.5-fold more Acot9 protein compared with healthy obese controls (Fig. 1C). These observations were in line with reports that the expression of Acots, including Acot9, is controlled by the peroxisome proliferator-activated receptor α in oxidative tissues.[13]

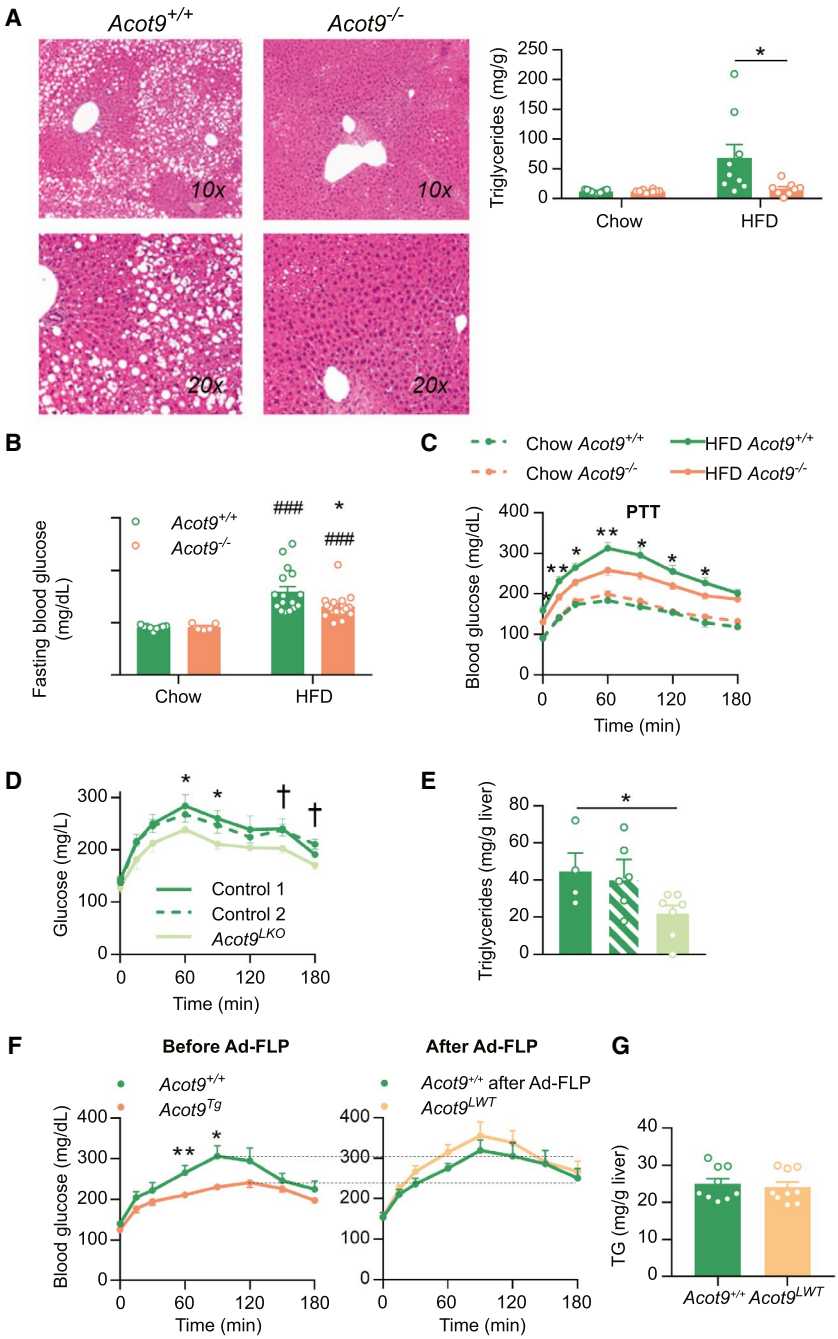

FIG. 2. Hepatic Acot9 expression promotes hepatic steatosis and HGP. 4-week-old mice were fed chow (*Acot9*$^{+/+}$, n = 11; *Acot9*$^{-/-}$, n = 11) or HFD (*Acot9*$^{+/+}$, n = 7; *Acot9*$^{-/-}$, n = 9) for 11 weeks. (A) Liver sections were subjected to hematoxylin and eosin staining and TG content measured. (B) Fasting (16 hours) blood glucose concentration. (C) Pyruvate tolerance test (PTT) following 16 hours fast. (D,E) Liver-specific deletion of Acot9 expression (*Acot9*^{LKO}, n = 8) was achieved by injecting 5-week-old *Acot9*$^{+/+}$ mice retro-orbitally with aav8-Tbg-iCre (5×10^{10} plaque-forming units [PFU]/mouse). WT mice injected with aav8-Tbg-iCre (Control 1, n = 4) or *Acot9*$^{+/+}$ mice injected with aav8-Tbg-LacZ (Control 2, n = 8) served as controls. (D) PTT and (E) hepatic TG were measured following 6 weeks on HFD. (F,G) Liver-specific rescue of Acot9 expression in Acot9 knockout mice (*Acot9*^{LWT}, n = 8) was achieved by injecting HFD-fed (11 weeks) 15-week-old *Acot9*^{Tg} mice retro-orbitally with Ad-flp (1×10^{9} PFU/mouse). *Acot9*$^{+/+}$ mice injected with Ad-flp served as control (n = 8). (F) PTTs were performed immediately before and 2 weeks after Ad-flp injection. (G) Hepatic TG were measured following liver-specific rescue of Acot9 expression. Error bars represent SEM. *$P < 0.05$; **$P < 0.01$ versus *Acot9*$^{+/+}$; †$P < 0.05$ versus WT; $^{###}P < 0.001$ versus chow-fed mice. Abbreviations: *Acot9*^{LKO}, Mice with the deletion of Acot9 only in the liver; *Acot9*^{Tg}, Conditional-ready mice with the deletion of Acot9 in the whole body; *Acot9*^{LWT}, *Acot9*^{Tg} mice that expresses Acot9 only in the liver; LacZ, beta galatosidase; PTT, pyruvate tolerance test; TG, triglycerides.

Acot9$^{-/-}$ MICE ARE PROTECTED AGAINST HFD-INDUCED WEIGHT GAIN AND ADIPOSITY

To elucidate the biological function of Acot9 activity, we generated a transgenic mouse model with genetic ablation of Acot9 expression (*Acot9*$^{-/-}$). The removal of exons 4 and 5 introduced an early stop codon at the end of exon 3 and knocked out Acot9 expression in all tissues (Supporting Fig. S2A-C). Although the immunoblot analyses of Acot9 produced nonspecific bands at close molecular weights (Supporting Fig. S2B), the lack of Acot9 expression in *Acot9*$^{-/-}$ mice was confirmed by mass spectrometry analysis of tissue lysates. At the age of weaning, *Acot9*$^{-/-}$ mice did not exhibit any discernible physical or developmental abnormalities and maintained identical growth curves compared with wild type (WT) littermates (*Acot9*$^{+/+}$) when fed chow diet (Fig. 1D). Suggestive of a role for Acot9 in diet-induced weight gain, *Acot9*$^{-/-}$ mice gained 16% less weight on HFD compared with *Acot9*$^{+/+}$ mice, with the weights diverging as early as 1 week into HFD (Fig. 1D). EchoMRI analysis of mice indicated that the reduced body weight was due to decreased adiposity because *Acot9*$^{-/-}$ mice exhibited similar lean mass but reduced fat mass compared with WT littermates (Fig. 1E). Reduced adiposity was due to a 26% reduction in the epididymal fat depots of HFD-fed *Acot9*$^{-/-}$ mice (Fig. 1F). The protection against adiposity was not due to reduced intake because food consumption did not differ between *Acot9*$^{+/+}$ and *Acot9*$^{-/-}$ mice (Fig. 1G).

HEPATIC Acot9 PROMOTES HFD-INDUCED HEPATIC STEATOSIS AND HGP

Similar to epididymal fat depots, high-fat feeding also increased lipid accumulation in the livers of *Acot9*$^{+/+}$ mice as determined by histology (Fig. 2A). However, *Acot9*$^{-/-}$ mice were protected against HFD-induced steatosis, which was associated with 77% reduction in the concentration of triglycerides (TG) in the livers of *Acot9*$^{-/-}$ mice following HFD (Fig. 2A), whereas hepatic concentrations of NEFA, phospholipids, and cholesterol remained unchanged (Supporting Fig. S3). We next monitored plasma lipids to determine whether reduced adiposity and hepatic TG storage were linked to changes in circulating lipids. Plasma TG, NEFA, cholesterol, and phospholipids remained unchanged between *Acot9*$^{+/+}$ and *Acot9*$^{-/-}$ mice following chow or HFD (Supporting Fig. S4).

We assessed whether the decreased hepatic TG accumulation in *Acot9*$^{-/-}$ mice was accompanied by improved glucose homeostasis. Glucose tolerance and insulin sensitivity were not affected by the loss of Acot9 expression, as determined by tolerance tests to glucose and insulin (Supporting Fig. S5A,B). However, the loss of Acot9 expression resulted in reduced fasting blood glucose (28%) in HFD-fed but not chow-fed mice (Fig. 2B), which was not attributable to increased plasma insulin (Supporting Fig. S5C). Because fasting plasma glucose is maintained by HGP, we used a pyruvate tolerance test to determine whether the activity of Acot9 contributed to HGP. The loss of Acot9 resulted in 15% reduction in HGP following HFD but not chow diet (Fig. 2C). Because the loss of Acot9 expression was not compensated by the increased expression of other Acot family members in the livers of *Acot9*$^{-/-}$ mice (Supporting Fig. S6A,B), the observed effects were most likely due to the loss of Acot9 thioesterase activity.

To elucidate whether Acot9 expression within hepatocytes directly controlled HGP and lipid accumulation, we first tested the role of Acot9 in HGP using primary hepatocytes and found that *Acot9*$^{-/-}$ hepatocytes produced 30% less glucose (Supporting Fig. S7). To further validate that the observed effects in mice were due to Acot9 expression within the hepatocytes, we generated mice with genetic ablation of Acot9 only in the hepatocytes (*Acot9*^{LKO}) by injecting the conditional ready *Acot9*$^{+/+}$ mice with aav8-Tbg-iCre, an adeno-associated virus that expresses Cre recombinase under the control of the hepatocyte-specific promoter of human thyroxine binding globulin (Tbg) (Supporting Fig. S8A-C). Residual Acot9 expression was hardly detectable in the livers of *Acot9*^{LKO} mice because of either Acot9 expression within nonparenchymal cells or incomplete recombination (Supporting Fig. S8B). Nonetheless, the severe loss of Acot9 expression only in the hepatocytes protected mice against HFD-induced increases in HGP and steatosis (Fig. 2D,E) without affecting body weight (Supporting Fig. S9). To complement the *Acot9*^{LKO} mouse model, we generated another transgenic mouse model whereby the global deletion of Acot9 expression was rescued only in the livers of HFD-fed adult mice (*Acot9*^{LWT}). This was achieved using a knockout-first mouse model (*Acot9*^{Tg}),

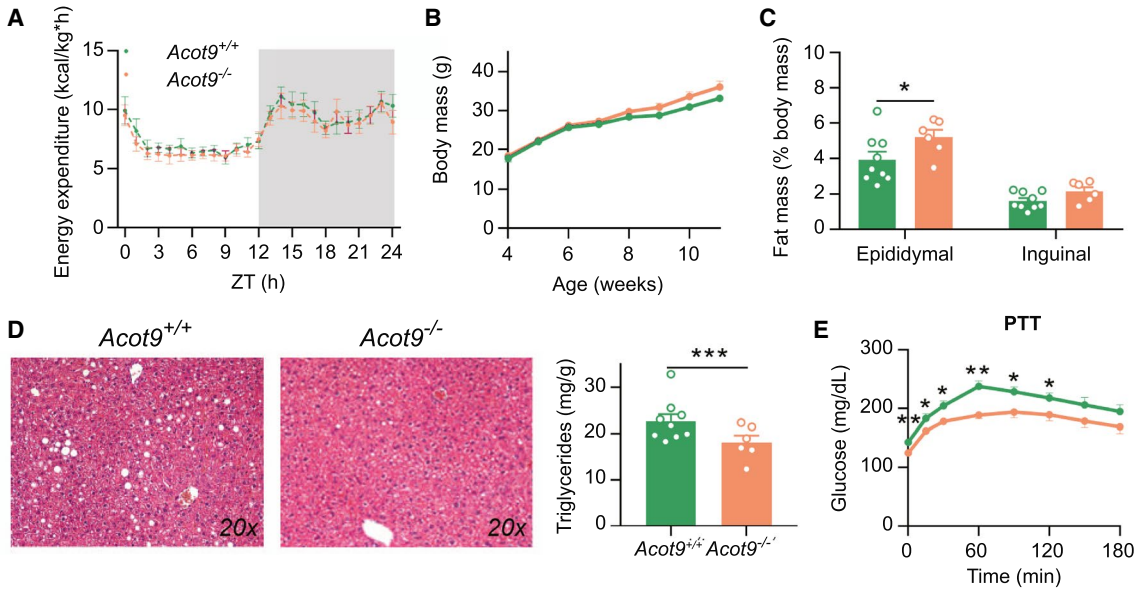

FIG. 3. The hepatic control of Acot9 is not secondary to adiposity. 4-week-old mice were fed HFD (*Acot9*$^{+/+}$, n = 8; *Acot9*$^{-/-}$, n = 8) at thermoneutrality (30°C) for 8 weeks. (A) EE was acquired through indirect calorimetry using the Promethion Metabolic Screening System and normalized to body weight. (B) Body weight curve. (C) Epididymal and inguinal fat depots were dissected and weighed. (D) Liver histology and TG. Liver TG were adjusted by analysis of covariance for fat mass (% body weight). (E) Pyruvate tolerance test (PTT) following 16-hour fast. Error bars represent SEM. *$P < 0.05$; **$P < 0.01$; ***$P < 0.001$ versus *Acot9*$^{+/+}$. Abbreviations: PTT, pyruvate tolerance test; ZT, zeitgeber time.

in which the whole-body Acot9 expression was disrupted by the insertion of an flippase recognition target (FRT)-flanked stop cassette (Supporting Fig. S8D). Hepatic Acot9 expression was rescued by injecting mice with adenovirus expressing flp recombinase (Ad-flp), which excised the FRT-flanked stop cassette in the livers but not in the heart or skeletal muscle as controls (Supporting Fig. S8E). The rescue of hepatic Acot9 expression did not only restore diet-induced increases in HGP (Fig 2F) but also reversed protection against hepatic steatosis (Fig 2G). For control, injection of WT littermates with Ad-flp did not affect HGP (Fig. 2F). Neither the loss nor the rescue of hepatic Acot9 affected hepatic concentrations of NEFA, phospholipids, and cholesterol (Supporting Fig. S10). Collectively, these findings indicate that the changes observed in HGP and steatosis are mechanistically attributable to the activity of Acot9 within the liver.

HEPATIC CONTROL BY Acot9 IS NOT SECONDARY TO ADIPOSITY

Two other Acot family members, Acot11 and Acot13, were shown to reduce energy expenditure (EE) by limiting thermogenesis.[14,15] Because Acot9 is also highly expressed in the thermogenic brown adipose tissue of mice (Supporting Fig. S2), we set to determine whether the protection of *Acot9*$^{-/-}$ mice against HFD-induced obesity was attributable to increased EE. We used metabolic cages to monitor the activity of *Acot9*$^{-/-}$ mice and measured EE by indirect calorimetry. The genetic ablation of Acot9 did not alter the ambulatory activity of mice following chow or HFD as determined by distance traveled over a 24-hour span (Supporting Fig. S11A). As anticipated, HFD feeding resulted in reduced oxygen consumption (VO_2), carbon dioxide production (VCO_2), and EE in *Acot9*$^{+/+}$ mice (Supporting Fig. S11B-D). Conversely, *Acot9*$^{-/-}$ mice maintained identical VO_2 rates and EE following chow or HFD, suggesting that Acot9 promotes HFD-induced reductions in oxygen and energy consumption (Supporting Fig. S11B-D). *Acot9*$^{-/-}$ mice also exhibited HFD-induced reductions in VCO_2 but to a lesser extent compared with WT littermates (Supporting Fig. S11C). This resulted in unchanged respiratory exchange ratio between *Acot9*$^{+/+}$ and *Acot9*$^{-/-}$ mice, indicating that reduced adiposity of

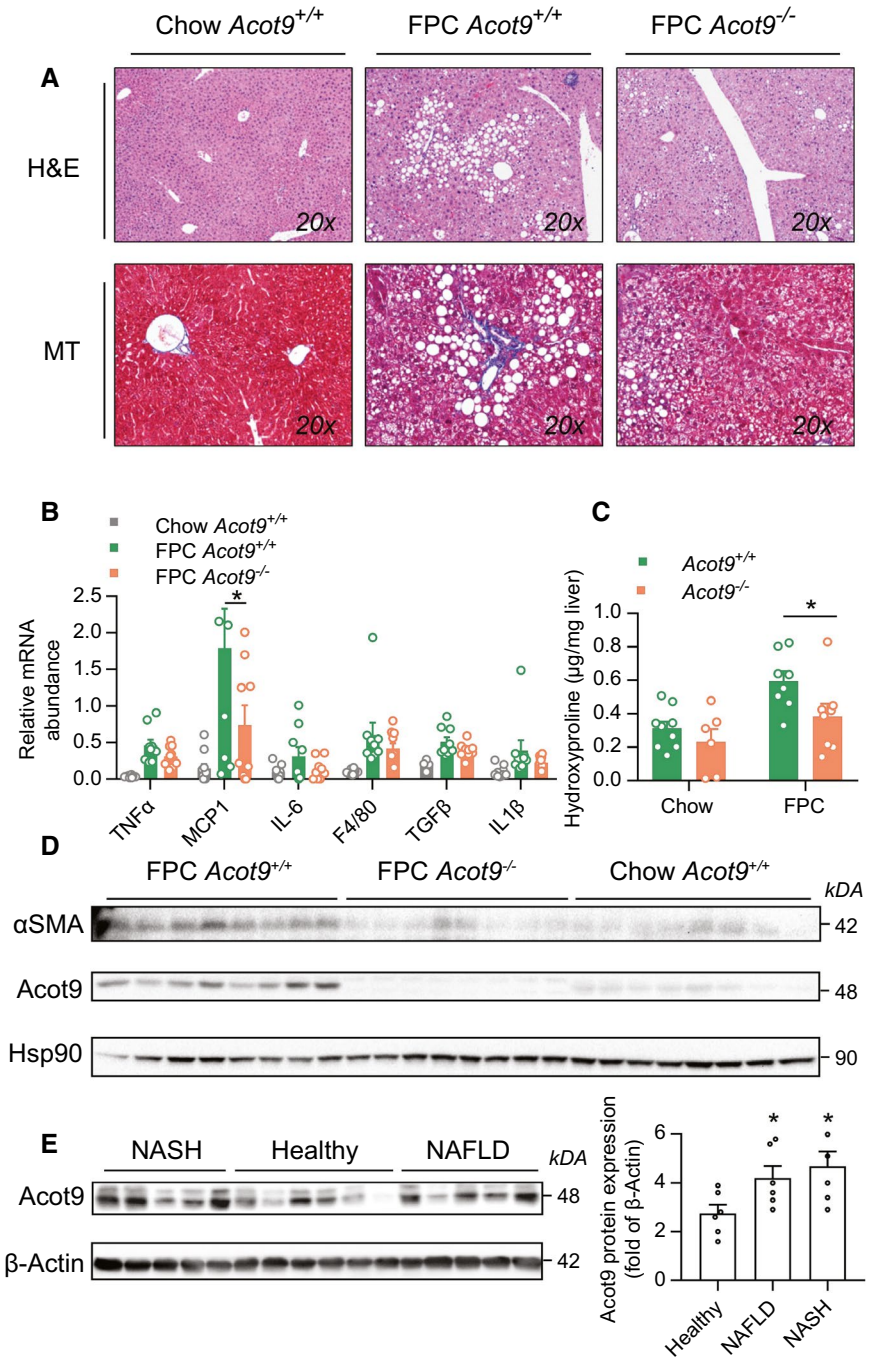

FIG. 4. Acot9 contributes to NASH. 4-week-old mice were fed FPC diet (*Acot9*$^{+/+}$, n = 8; *Acot9*$^{-/-}$, n = 10) for 16 weeks. Chow-fed *Acot9*$^{+/+}$ mice (n = 8) served as baseline. (A) Liver sections were subjected to hematoxylin and eosin (H&E) staining for steatosis and Masson's trichrome (MT) staining for fibrosis. (B) Hepatic expression of inflammatory markers as determined by quantitative real-time PCR analysis using β-actin as internal control. (C) Hepatic hydroxyproline content was measured and normalized to liver mass. (D) Hepatic expression of alpha smooth muscle actin (αSMA) was determined by immunoblot analysis using heat shock protein 90 (Hsp90) as internal control. (E) Immunoblot analysis of Acot9 expression in obese human livers with simple steatosis or fibrosis (NASH) compared with metabolically healthy controls (body mass index > 36). Inset barplot represent densitometry analyses normalized to β-actin as loading control. Error bars represent SEM. **P* < 0.05 versus control or *Acot9*$^{+/+}$. Abbreviations: IL, interleukin; MCP1, monocyte chemoattractant protein 1; TGFβ, tumor growth factor beta; TNFα, tumor necrosis factor alpha.

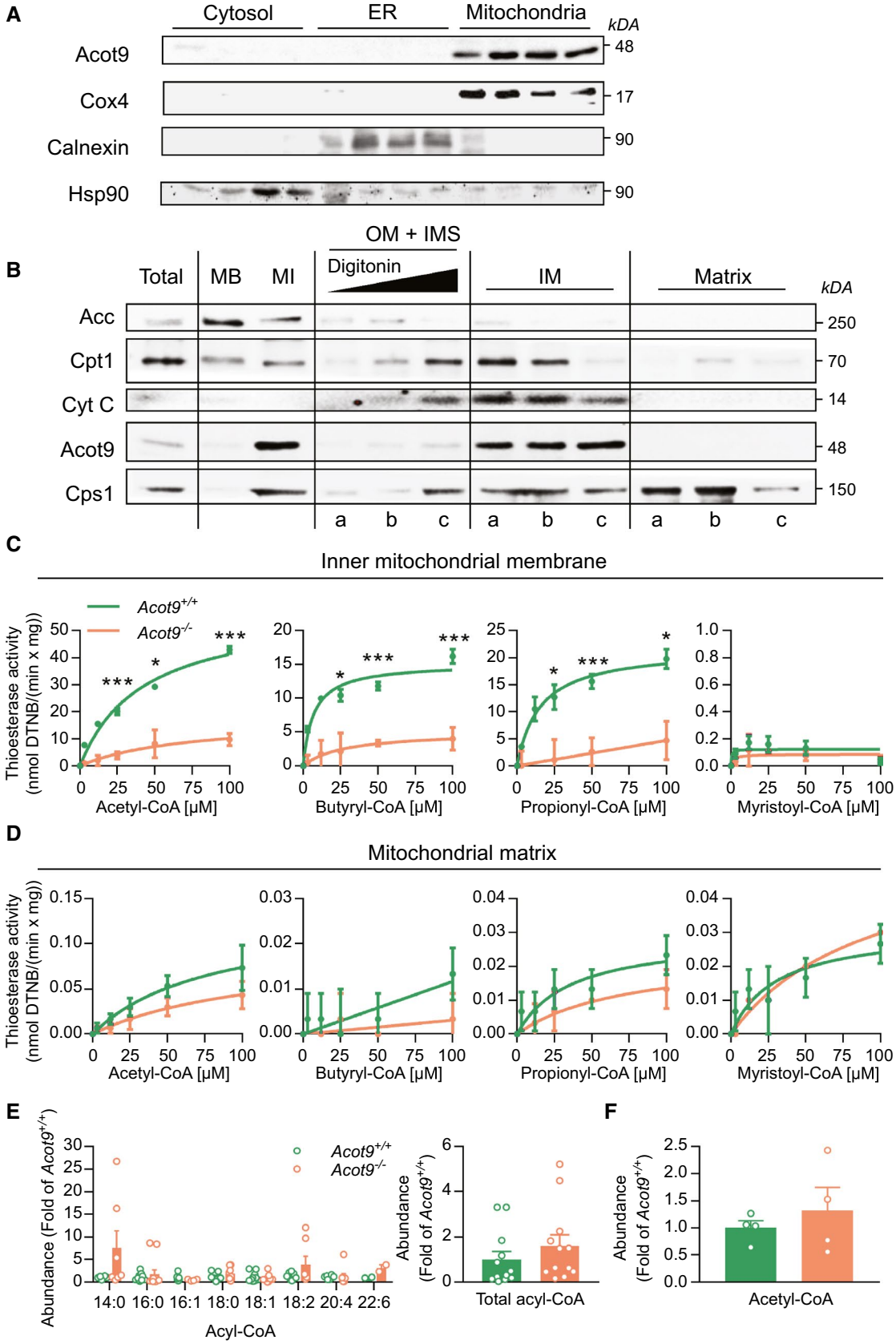

FIG. 5. Subcellular localization and enzymatic activity of Acot9 in the livers of mice. Subcellular compartments of livers from HFD-fed *Acot9*$^{+/+}$ and *Acot9*$^{-/-}$ mice were fractionated by centrifugation. (A) Immunoblot analysis of Acot9 using subcellular markers for cytosol (heat shock protein 90 [Hsp90]), ER (Calnexin), and mitochondria (cytochrome *c* oxidase 4 [Cox4]). (B) Immunoblot analysis of mitochondrial fractions: mitochondria-bound (MB) proteins were separated from mitochondria-integrated (MI) proteins using sodium carbonate. Whole mitochondria were digested with either (a) 0.2, (b) 1, or (c) 5 mg/mL digitonin to lyse the OM of the mitochondria, gradually exposing proteins from OM to the IMS. Following each digitonin treatment, remaining mitoplast pellets were fractionated into IM and matrix compartments by centrifugation. Mitochondrial fraction markers: Acetyl-CoA carboxylase (ACC; MB), carnitine palmitoyltransferase 1 (Cpt1; MI), Cyt C (IMS + IM), carbamoyl phosphate synthetase 1 (Cps1; matrix). (C,D) Thioesterase activity of (C) IM and (D) matrix proteins on exogenous acyl-CoA substrates. (E) Abundance of acyl-CoA molecular species in HFD-fed mice was determined by mass spectrometry-based lipidomics (n = 4-12). Inset bar graph represents total acyl-CoA. (F) Abundance of hepatic acetyl-CoA was determined by mass spectrometry-based metabolomics (*Acot9*$^{+/+}$, n = 4; *Acot9*$^{-/-}$, n = 4). Error bars represent SEM. $^{*}P < 0.05$; $^{***}P < 0.001$ versus *Acot9*$^{+/+}$. Abbreviation: DTNB, 5,5′-dithiobis-(2-nitrobenzoic acid).

Acot9$^{-/-}$ mice was not attributable to increased systemic preference for lipids as an energy source compared with carbohydrates (Supporting Fig. S11E).

To determine whether increased EE of *Acot9*$^{-/-}$ mice was due to increased utilization of energy toward thermogenesis, we housed *Acot9*$^{+/+}$ and *Acot9*$^{-/-}$ mice at thermoneutrality (30°C) for 8 weeks. Removal of the thermogenic burden equalized the EE of *Acot9*$^{+/+}$ and *Acot9*$^{-/-}$ mice (Fig. 3A). Under these circumstances, *Acot9*$^{-/-}$ mice were not protected against HFD-induced weight gain and adiposity (Fig. 3B,C). Although *Acot9*$^{-/-}$ mice accumulated 24% more epididymal fat at thermoneutrality (Fig. 3C), they were still protected against HFD-induced hepatic steatosis (Fig. 3D). We also found that *Acot9*$^{-/-}$ mice maintained reduced fasting plasma glucose and HGP even in the presence of increased epididymal adiposity (Fig. 3E). These results indicate that the regulation of HGP and steatosis by hepatic Acot9 expression is not secondary to decreased adiposity of *Acot9*$^{-/-}$ mice.

METABOLIC CONTROL BY Acot9 EXACERBATES STEATOHEPATITIS

Hepatic steatosis is the primary risk factor for the pathogenesis of nonalcoholic steatohepatitis (NASH). To determine the role of metabolic regulation by Acot9 in susceptibility to NASH, we subjected mice to a fibrogenic diet rich in fructose, palmitate, and cholesterol (FPC).[16] Compared with chow diet, FPC diet did not induce excessive weight gain in either *Acot9*$^{+/+}$ or *Acot9*$^{-/-}$ mice (Supporting Fig. S12) but promoted hepatic steatosis, inflammation, and fibrosis (Fig. 4). Similar to our observations using HFD, the loss of Acot9 protected mice against FPC-induced macrovesicular steatosis (Fig. 4A). In the absence of Acot9, the livers of mice tended to express reduced markers of inflammation with significant reductions (3.7-fold) in monocyte chemoattractant protein 1, which orchestrates the infiltration of liver by macrophages and monocytes during the pathogenesis of NASH (Fig. 4B).[17] The role of metabolic control by Acot9 in exacerbating fibrosis was supported by reductions in FPC-induced increases in hydroxyproline (1.6-fold, Fig. 4C) and alpha smooth muscle actin in the livers of *Acot9*$^{-/-}$ mice compared with *Acot9*$^{+/+}$ mice (Fig. 4D). Although FPC-induced inflammation and fibrosis were more evident at the molecular level, the pathology of livers failed to identify the lobular inflammation and ballooning that is commonly observed in human NASH (Supporting Table S1). Nonetheless, NAFLD activity scores (NAS)[18,19] still implicated Acot9 in FPC-induced steatosis (Supporting Table S1). Furthermore, Acot9 was expressed equally in the livers of patients with obesity who had NAFLD and NASH (Fig. 4E), suggesting that Acot9 most likely promotes the metabolic first-hit but not the progression of simple steatosis to steatohepatitis.

Acot9 LOCATES TO THE INNER MEMBRANE OF THE MITOCHONDRIA AND REGULATES THE ACTIVITY OF SHORT-CHAIN FATTY ACIDS

To determine the mechanisms by which hepatic Acot9 regulates HGP and steatosis, we determined the subcellular localization and thioesterase activity of Acot9. Subcellular fractionation of livers confirmed Acot9 as a mitochondrial protein as described[10] (Fig. 5A). Acot9 expression was absent in the subcellular fractions that lacked mitochondrial

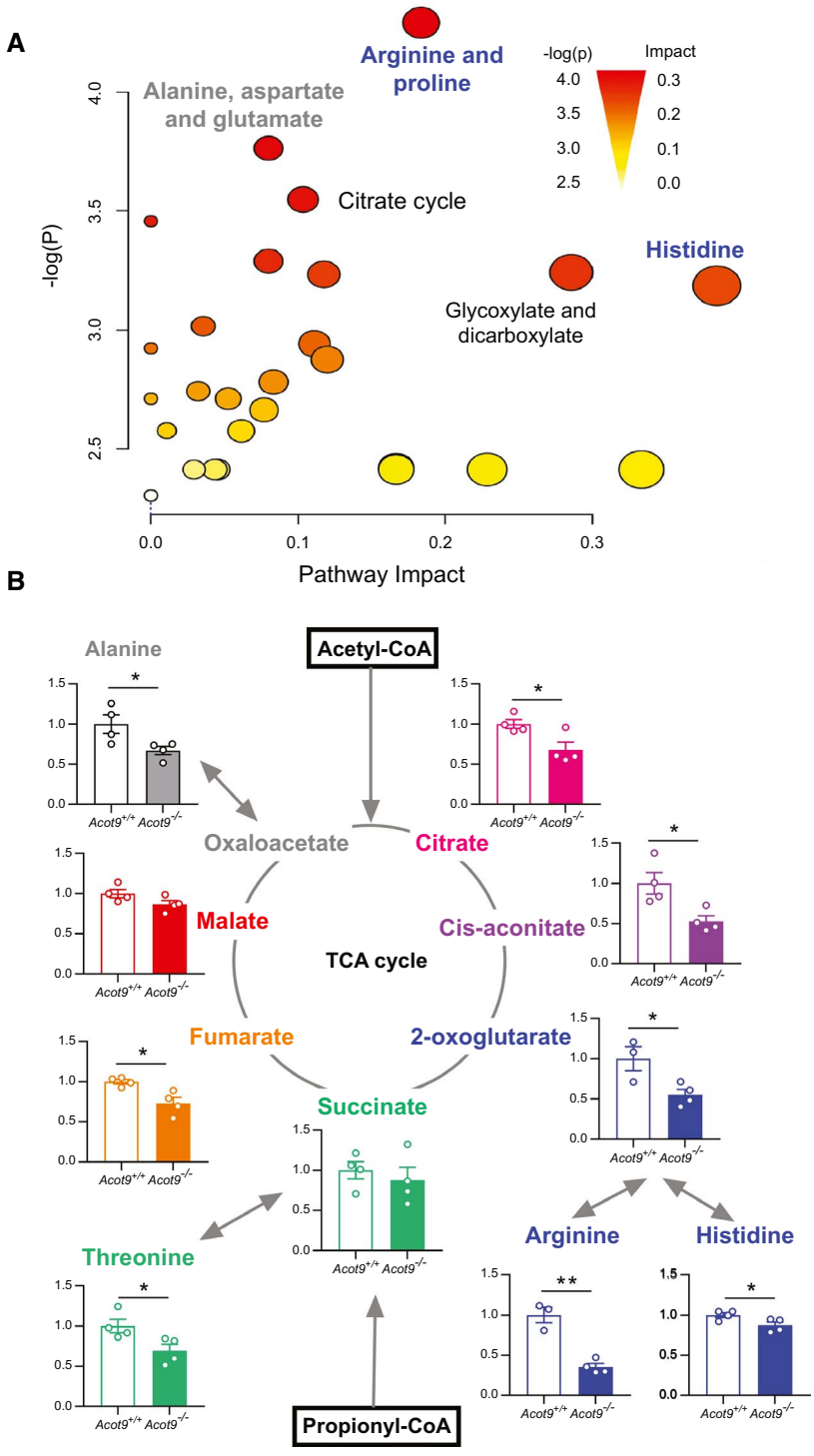

FIG. 6. Livers of *Acot9*$^{-/-}$ mice have decreased TCA cycle metabolites. 4-week-old mice were fed HFD (*Acot9*$^{+/+}$, n = 7; *Acot9*$^{-/-}$, n = 9) for 9 weeks and fasted 16 hours before mass spectrometry-based metabolomics. (A) Schematic representation of the pathway analysis performed on the metabolomics data using MetaboAnalyst. (B) Relative concentrations of select TCA cycle metabolites (*y* axis represents fold of *Acot9*$^{+/+}$). **P* < 0.05; ***P* < 0.01 versus *Acot9*$^{+/+}$.

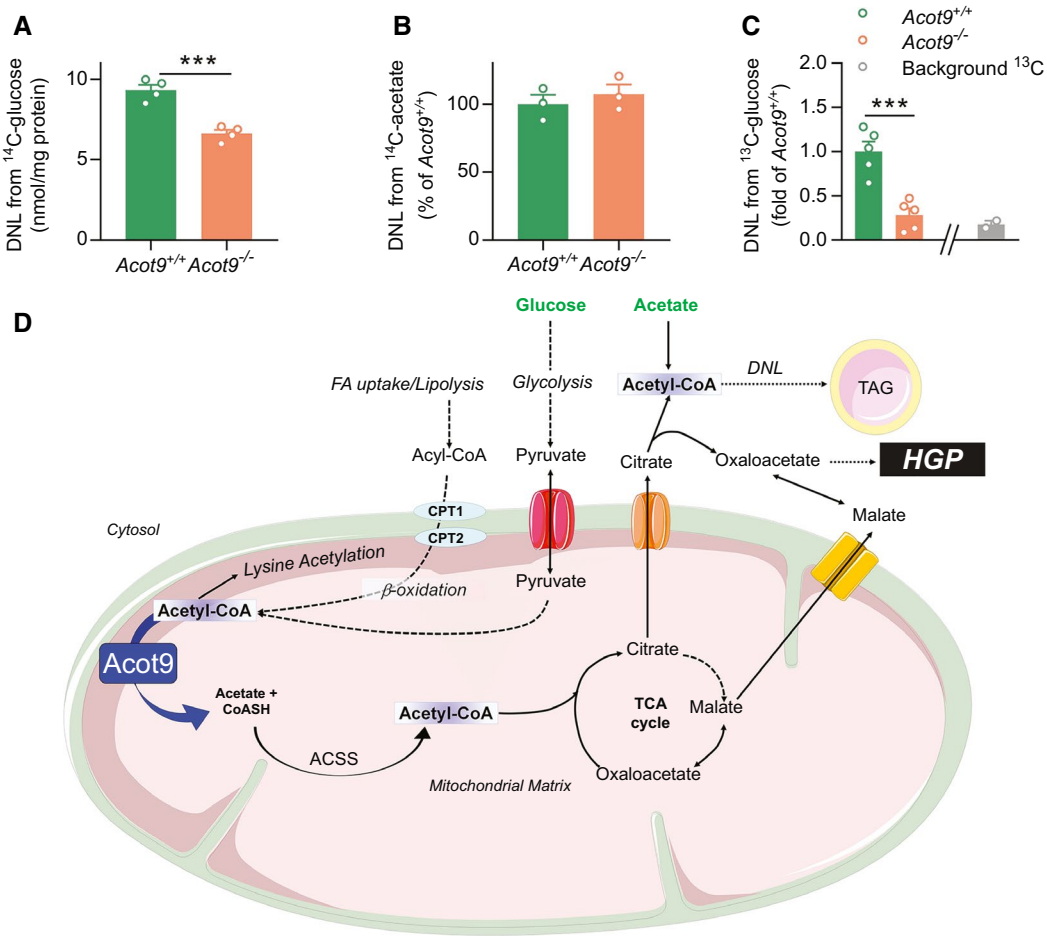

FIG. 7. Acot9 traffics mitochondrial acetyl-CoA toward DNL and HGP. (A,B) Rates of DNL from (A) [^{14}C]-glucose and (B) [^{14}C]-acetate was measured in primary hepatocytes (n = 4). (C) ^{13}C enrichment in hepatic lipids was determined by 2D-NMR after supplying mice (n = 5) with ^{13}C-glucose in drinking water (12% wt/vol for 24 hours). Background ^{13}C barplot represents naturally occurring abundance of ^{13}C in the hepatic lipids of *Acot9*$^{+/+}$ mice that were not given ^{13}C-glucose. Error bars represent SEM. ***P < 0.001 versus *Acot9*$^{+/+}$. (D) Proposed model for the role of Acot9 in lipid and glucose biosynthesis. Acetyl-CoA in the mitochondrial matrix originate from (1) biosynthesis from metabolites such as pyruvate, (2) oxidation end-product of even-chain fatty acyl-CoA, which represents more than 99% of total β-oxidation, and (3) re-esterification of acetate to CoASH by acetyl-CoA synthetases (ACSS). Acetyl-CoA cannot be transported from the matrix into the cytosol and will be used for either lysine acetylation of proteins or enter the TCA cycle for the production of citrate, which can be transported into the cytosol to be used as a substrate for lipogenesis. Another product of the TCA cycle, oxaloacetate, becomes a substrate for HGP. Acot9 sustains the TCA cycle flux by deactivating acetyl-CoA at the inner mitochondrial membrane, limiting its use for lysine acetylation and sequestering acetate to the mitochondrial matrix, where it can enter the TCA cycle after re-esterification to acetyl-CoA by ACSS family members that are located in the mitochondrial matrix. Abbreviations: ACSS, Acyl-CoA synthetase short-chain family member; CPT, Carnitine palmitoyltransferase; FA, fatty acid; HGP, hepatic glucose production; TAG, triacylglycerol.

proteins but contained ER or cytosolic proteins (Fig. 5A). Further fractionation of the mitochondrial compartments located Acot9 specifically to the inner mitochondrial membrane (Fig. 5B): Sodium carbonate treatment of whole mitochondria washed away the majority of mitochondria-bound proteins, such as acetyl-CoA carboxylase (ACC),[20] whereas Acot9 remained among mitochondria-integrated proteins (Fig. 5B). Digestion of the mitochondria with increasing concentrations of digitonin gradually cleared out ACC and revealed proteins that are either imbedded in the outer membrane (OM), such as carnitine palmitoyltransferase 1,[21] or reside within the intermembrane space (IMS) and the outer surface of the inner membrane (IM), such as cytochrome C (Cyt C).[22] Acot9 was not present in

these fractions (Fig. 5B, OM + IMS) and resided in the remaining mitoplasts, which consist of IM and matrix compartments. Further fractionation of the mitoplasts localized Acot9 only to the IM compartment where Cyt C was also highly abundant because of its interactions with the electron transport chain (Fig. 5B).[22] Only carbamoyl phosphate synthetase 1,[23] which controls the urea cycle in the matrix, was strongly associated with the matrix fraction (Fig. 5B). Thioesterase activity assays of mitochondrial fractions indicated that Acot9 specifically targets short-chain acyl-CoA within the inner mitochondrial membrane (Fig. 5C) but not other mitochondrial fractions, including the matrix (Fig. 5D). We next determined whether this activity of Acot9 altered the acyl-CoA landscape within the livers of mice. Lipidomics of whole livers did not reveal a difference in total or specific acyl-CoA species, indicating that Acot9 regulates trafficking of short-chain acyl-CoA at the inner mitochondrial membrane but not overall abundance of the active acyl-CoA pool (Fig. 5E,F).

Acot9 PROMOTES HFD-INDUCED LIVER DISEASE BY INCREASING SUBSTRATE AVAILABILITY FOR DNL AND HGP

Mitochondrial anaplerosis is the nonoxidative flux of intermediates into the TCA cycle, which contributes to lipogenesis and gluconeogenesis by increasing the availability of lipogenic and gluconeogenic substrates. Metabolomics analysis of whole livers revealed that the greatest divergence between *Acot9*$^{+/+}$ and *Acot9*$^{-/-}$ mice was among metabolites that are associated with the TCA cycle (Fig. 6A, Supporting Table S2). The loss of Acot9-mediated deactivation of short-chain fatty acids (SCFA), including acetyl-CoA and propionyl-CoA, at the inner mitochondrial membrane resulted in the reduction of prominent metabolites of the TCA cycle, such as citrate (32%), cis-aconitate (47%), 2-oxoglutarate (45%), and fumarate (27%), as well as several amino acids that are interchangeable with the TCA cycle, such as alanine (33%), arginine (67%), histidine (13%), and threonine (31%) (Fig. 6B). These reductions were not secondary to Acot9-mediated changes in the regulation of TCA flux by citrate synthase activity (Supporting Fig. S13).

To test whether Acot9 promotes steatosis by facilitating the production of citrate from the TCA cycle, we induced DNL in primary hepatocytes using glucose as a substrate (Fig. 7A,D). Acetyl-CoA that originates from glycolysis within the mitochondria depended on the activity of Acot9 before being incorporated into citrate for DNL (Fig. 7A). By contrast, Acot9 did not exert regulatory control over cytosolic acetyl-CoA that originated from exogenous acetate (Fig. 7B,D). To determine whether Acot9 traffics acetyl-CoA to DNL *in vivo*, we supplied mice with drinking water containing [$^{13}C_1$]-D-glucose and measured its incorporation into lipids in the livers of mice using two-dimensional nuclear magnetic resonance (2D-NMR) spectroscopy (Supporting Fig. S14). Similar to our observations in hepatocytes, the loss of Acot9 expression resulted in 72% reduction in the incorporation of dietary glucose into newly synthesized lipids (Fig. 7C). Considering that the endogenous supply of acetyl-CoA in hepatocytes originates from the mitochondria, these findings support a maladaptive mechanism whereby increased Acot9 activity in the mitochondria promotes the bioavailability of acetyl-CoA for DNL in the setting of overnutrition (Fig. 7D).

We next investigated pathways other than TCA where SCFA can be trafficked in the absence of Acot9. We found that the acetyl-CoA molecules that were trafficked away from the TCA cycle were most likely used in the acylation of hepatic proteins: the loss of Acot9 resulted in the acetylation of a distinct set of proteins in the livers of mice (Supporting Fig. S15A). This was directly mediated by the activity of Acot9 within the liver because the hepatic rescue of Acot9 expression in *Acot9*^{LWT} mice completely reversed the increased acetylation of these target proteins (Supporting Fig. S15B).

To exclude other metabolic pathways by which the activity of Acot9 can influence hepatic TG accumulation, we measured fatty acid uptake and oxygen consumption (OCR) in primary hepatocytes, β-oxidation in liver homogenates, and VLDL secretion rates in mice. The Acot9-mediated accumulation of hepatic TG was not secondary to changes in the rates of hepatic fatty acid uptake, OCR, β-oxidation, and VLDL secretion (Supporting Fig. S16A-D). In

the absence of citrate as a lipogenic substrate, livers of *Acot9*$^{-/-}$ mice exhibited reduced expression of genes that promote lipogenesis such as Fas (0.6-fold) and ACC (0.7-fold). ACC activity was also suppressed by increased phosphorylation (Supporting Fig. S16E-G). Furthermore, cell death-inducing DNA fragmentation factor alpha-like effector A (cidea), which promotes liver steatosis by promoting the fusion of lipid droplets in the setting of obesity,[24] was down-regulated in the livers of *Acot9*$^{-/-}$ mice (0.6-fold; Supporting Fig. S16E). On the other hand, the expression of genes that regulate fatty acid uptake, oxidation, TG synthesis, and catalysis remained unchanged (Supporting Fig. S16E-G).

We next excluded the contributions of gluconeogenic factors as well as glycogen mobilization in the regulation of fasting plasma glucose by Acot9. Hepatic expression of hepatocyte nuclear factor 4 alpha, forkhead box O1, peroxisome proliferator-activated receptor gamma coactivator 1-alpha, phosphoenolpyruvate carboxykinase, and glucose-6 phosphatase did not differ between the genotypes, indicating that the suppression of HGP in *Acot9*$^{-/-}$ mice was not secondary to transcriptional regulation (Supporting Fig. S17A). We further determined whether decreased fasting blood glucose was due to reduced glycogenolysis because glycogen can contribute up to half of circulating glucose under fasting conditions.[25] However, hepatic glycogen stores and free glucose concentrations were not altered in *Acot9*$^{-/-}$ mice, suggesting that the decreased HGP was not due to a lack of glycogen mobilization by Acot9 (Supporting Fig. S17B).

Discussion

This study was designed to gain insight into the biological role of Acot9. Acot9 expression is directly associated with the pathogenesis of NAFLD in mice and patients with obesity. In support of a maladaptive role for increased Acot9 activity, the loss of Acot9 in mice protected against diet-induced steatosis and excessive HGP. Biologically, Acot9 played a central role in the deactivation of hepatic SCFA, as evidenced by increased K_m (affinity) for the hydrolysis of acetyl-CoA, butyryl-CoA, and propionyl-CoA but not long-chain fatty acids (LCFA) in the livers of *Acot9*$^{-/-}$ mice. Because β-oxidation and the production of ketone bodies mostly depend on LCFA, these functions were not affected by Acot9. Instead, strategic biochemical assays and metabolomics analysis strongly indicated that the activity of Acot9 toward SCFA must have increased TCA flux, which in turn provided substrates for DNL and HGP. Taken together, our findings support a molecular mechanism whereby increased Acot9 activity drives steatosis by channeling acyl-CoAs to lipogenesis and HGP under the pathophysiology of obesity (Fig. 7D).

Among hepatic SCFA, only acetyl-CoA was detectable by mass spectrometry analysis (Fig. 6) because resting mitochondrial abundance of butyryl-CoA and propionyl-CoA are significantly low. Butyryl-CoA is further oxidized to acetyl-CoA, and propionyl-CoA is the final product of odd-chain fatty acid oxidation, which represents less than 1% of total β-oxidation.[26] This indicates that, although Acot9 exhibited activity toward a broad array of SCFA *in vitro*, its biological impact was based on the deactivation of acetyl-CoA at the IM of the mitochondria (Fig. 7D).

The hallmark of NAFLD is the ectopic lipid accumulation in the form of TG,[27] for which the source of fatty acids originates from circulating NEFA (60%), DNL (25%), and dietary chylomicrons (15%).[28] Hepatic fatty acid uptake is directly proportional to circulating NEFA.[29] Arguing against a role for circulating NEFA in Acot9-mediated steatosis, the concentration of plasma NEFA and hepatic fatty acid uptake rates did not differ between *Acot9*$^{+/+}$ and *Acot9*$^{-/-}$ mice. Instead, the loss of Acot9 resulted in reduced activation of the lipogenic machinery at the level of substrate availability. A lack of evidence for the inhibition of VLDL secretion further supported a central role for increased DNL in Acot9-mediated steatosis. The importance of DNL in the pathogenesis of NAFLD in humans is highlighted by a 3-fold increase in this pathway in patients with NAFLD.[30] The absence of Acot9 also decreased HGP in the setting of excessive nutrition. In humans, increases in liver TG are accompanied by increases in HGP (25%) and hepatic TCA cycle flux (50%).[31] In relevance to NAFLD in humans, reduced HGP in *Acot9*$^{-/-}$ mice was accompanied by reductions in hepatic TG concentrations and TCA cycle flux, which promotes gluconeogenesis through the production of gluconeogenic substrates such as oxaloacetate, adenosine triphosphate, and reduced nicotinamide adenine dinucleotide.[31] Reduced steatosis in the absence of Acot9 expression also protected mice against FPC

diet-induced exacerbation of steatosis and markers of inflammation and fibrosis. However, NAS analysis implicated Acot9 only in macrovesicular steatosis. In addition, the hepatic expression of Acot9 was not further exacerbated in humans with NASH compared with those with simple steatosis, which all together argue against a role of Acot9 in disease progression from simple steatosis to NASH.

In addition to trafficking SCFA toward anabolic pathways, Acot9 also limited acetyl-CoA supplies that are used for lysine acetylation of proteins (AcK). AcK represents one of the most important post-translational modifications in metabolic regulation[32] and increases in response to obesity in hepatic mitochondria.[33] This is driven by increased local acetyl-CoA concentrations, which initiate the nonenzymatic binding of acetyl-CoA to unprotonated lysine.[34] Therefore, local acetyl-CoA bioavailability plays an essential role in metabolic control. Our results indicate that Acot9-mediated deactivation of acetyl-CoA at the IM of mitochondria represents a mechanism of inhibition of AcK in addition to described mitochondrial deacetylases sirtuin (SIRT) 3 and SIRT4, which also play pivotal roles in metabolism.[33,35,36]

Reduced body weight gain in *Acot9*$^{-/-}$ mice was at least in part due to increased EE, which encompasses basal metabolic rate, thermogenesis, and the thermic effect of activity and food processing.[37] Because Acot9 expression did not alter food intake, physical activity, or substrate utilization, future studies will elucidate the role of Acot9 in thermogenesis and basal metabolic rate. Nonetheless, the study of weight-matched mice that were housed at thermoneutrality for 8 weeks eliminated contributions from Acot9 expression in thermogenic adipose tissue and solidified the role of hepatic Acot9 expression in promoting steatosis and gluconeogenesis independently from adiposity.

Mouse *Acot9* and *Acot10* were originally identified as a single polypeptide[38] because Acot9 and Acot10 have 97% and 96% homology at the transcript and protein level, respectively. A human orthologue for mouse *Acot10* does not exist. Mouse *Acot10*, which consists of a single exon, was shown to be a duplicated retrogene with no evidence of pseudogenization.[39] The hypothesis that *Acot10* originates from a transcript duplication of *Acot9* is also supported by the shared sequence identity within the first 169 nucleotides of the 5′ untranslated region (UTR; 95%) as well as the first 71 nucleotides of the 3′ UTR (100%) without any homology throughout the untranscribed flanks. Our results further supported the lack of Acot10 protein expression in mice.

In conclusion, we leveraged transgenic mouse models to delineate the biological functions of Acot9, particularly in the liver. Our results demonstrated important *in vivo* functions of a member of the Acot enzyme family in metabolic regulation. Considering that *Acot9*$^{-/-}$ mice are protected against diet-induced hepatic steatosis and HGP, the enzymatic activity of Acot9 in the liver could represent an attractive target for the management of NAFLD.

Acknowledgments: The authors thank Dr. Kaveh Ashrafi (University of California San Francisco) for providing RNAi library targeting Acot family members in Caenorhabditis elegans, and Stephanie A. Osganian (Massachusetts General Hospital) for her assistance with the human liver samples.

Author Contributions: S.S. contributed to the hypothesis, designed methodology and conducted experiments, contributed to data curation, formal analysis and wrote the manuscript. J.Q. designed methodology and conducted mouse experiments. Y.Z. conducted experiments and contributed to the generation of transgenic mouse models. K.M.M-S. designed and performed mass spectrometry experiments and analyzed data. N.K. designed methodology and conducted enzyme activity experiments. C.D.H. oversaw the metabolic monitoring of mice, analyzed data and reviewed manuscript. K.E.C. provided human liver samples and reviewed data. W.C.B. designed methodology and performed nuclear magnetic resonance experiments. E.A.O. supervised the mass spectrometry analysis of lipids, reviewed and edited the manuscript. B.A.E. conceptualized the hypothesis, directed and validated the work, designed methodology, performed experiments, analyzed data and wrote the manuscript. All authors approve the final version of the manuscript.

REFERENCES

1) Younossi Z, Anstee QM, Marietti M, Hardy T, Henry L, Eslam M, et al. Global burden of NAFLD and NASH: trends, predictions, risk factors and prevention. Nat Rev Gastroenterol Hepatol 2018;15:11-20.
2) Machado MV, Cortez-Pinto H. Non-alcoholic fatty liver disease: what the clinician needs to know. World J Gastroenterol 2014;20:12956-12980.

3) Ipsen DH, Lykkesfeldt J, Tveden-Nyborg P. Molecular mechanisms of hepatic lipid accumulation in non-alcoholic fatty liver disease. Cell Mol Life Sci 2018;75:3313-3327.
4) Tillander V, Alexson SEH, Cohen DE. Deactivating fatty acids: acyl-CoA thioesterase-mediated control of lipid metabolism. Trends Endocrinol Metab 2017;28:473-484.
5) Grevengoed TJ, Klett EL, Coleman RA. Acyl-CoA metabolism and partitioning. Annu Rev Nutr 2014;34:1-30.
6) Birkenfeld AL, Shulman GI. Nonalcoholic fatty liver disease, hepatic insulin resistance, and type 2 diabetes. Hepatology 2014;59:713-723.
7) Kawano Y, Ersoy BA, Li Y, Nishiumi S, Yoshida M, Cohen DE. Thioesterase superfamily member 2 (Them2) and phosphatidylcholine transfer protein (PC-TP) interact to promote fatty acid oxidation and control glucose utilization. Mol Cell Biol 2014;34:2396-2408.
8) Ersoy BA, Maner-Smith KM, Li Y, Alpertunga I, Cohen DE. Thioesterase-mediated control of cellular calcium homeostasis enables hepatic ER stress. J Clin Invest 2018;128:141-156.
9) Alves-Bezerra M, Li Y, Acuna M, Ivanova AA, Corey KE, Ortlund EA, et al. Thioesterase superfamily member 2 promotes hepatic VLDL secretion by channeling fatty acids into triglyceride biosynthesis. Hepatology 2019;70:496-510.
10) Tillander V, Arvidsson Nordstrom E, Reilly J, Strozyk M, Van Veldhoven PP, Hunt MC, et al. Acyl-CoA thioesterase 9 (ACOT9) in mouse may provide a novel link between fatty acid and amino acid metabolism in mitochondria. Cell Mol Life Sci 2014;71:933-948.
11) Ersoy BA, Tarun A, D'Aquino K, Hancer NJ, Ukomadu C, White MF, et al. Phosphatidylcholine transfer protein interacts with thioesterase superfamily member 2 to attenuate insulin signaling. Sci Signal 2013;6:ra64.
12) Mullaney BC, Ashrafi KC. C. elegans fat storage and metabolic regulation. Biochim Biophys Acta 2009;1791:474-478.
13) Patsouris D, Reddy JK, Muller M, Kersten S. Peroxisome proliferator-activated receptor alpha mediates the effects of high-fat diet on hepatic gene expression. Endocrinology 2006;147:1508-1516.
14) Zhang Y, Li Y, Niepel MW, Kawano Y, Han S, Liu S, et al. Targeted deletion of thioesterase superfamily member 1 promotes energy expenditure and protects against obesity and insulin resistance. Proc Natl Acad Sci U S A 2012;109:5417-5422.
15) Kang HW, Ozdemir C, Kawano Y, LeClair KB, Vernochet C, Kahn CR, et al. Thioesterase superfamily member 2/Acyl-CoA thioesterase 13 (Them2/Acot13) regulates adaptive thermogenesis in mice. J Biol Chem 2013;288:33376-33386.
16) Wang X, Zheng Z, Caviglia JM, Corey KE, Herfel TM, Cai B, et al. Hepatocyte TAZ/WWTR1 promotes inflammation and fibrosis in nonalcoholic steatohepatitis. Cell Metab 2016;24:848-862.
17) Deshmane SL, Kremlev S, Amini S, Sawaya BE. Monocyte chemoattractant protein-1 (MCP-1): an overview. J Interferon Cytokine Res 2009;29:313-326.
18) Kleiner DE, Brunt EM, Van Natta M, Behling C, Contos MJ, Cummings OW, et al. Design and validation of a histological scoring system for nonalcoholic fatty liver disease. Hepatology 2005;41:1313-1321.
19) Boland ML, Oldham S, Boland BB, Will S, Lapointe JM, Guionaud S, et al. Nonalcoholic steatohepatitis severity is defined by a failure in compensatory antioxidant capacity in the setting of mitochondrial dysfunction. World J Gastroenterol 2018;24:1748-1765.
20) Monteuuis G, Suomi F, Keratar JM, Masud AJ, Kastaniotis AJ. A conserved mammalian mitochondrial isoform of acetyl-CoA carboxylase ACC1 provides the malonyl-CoA essential for mitochondrial biogenesis in tandem with ACSF3. Biochem J 2017;474:3783-3797.
21) Broadway NM, Pease RJ, Birdsey G, Shayeghi M, Turner NA, David SE. The liver isoform of carnitine palmitoyltransferase 1 is not targeted to the endoplasmic reticulum. Biochem J 2003;370:223-231.
22) Kirkinezos IG, Bacman SR, Hernandez D, Oca-Cossio J, Arias LJ, Perez-Pinzon MA, et al. Cytochrome c association with the inner mitochondrial membrane is impaired in the CNS of G93A-SOD1 mice. J Neurosci 2005;25:164-172.
23) Park MJ, D'Alecy LG, Anderson MA, Basrur V, Feng Y, Brady GF, et al. Constitutive release of CPS1 in bile and its role as a protective cytokine during acute liver injury. Proc Natl Acad Sci U S A 2019;116:9125-9134.
24) Xu W, Wu L, Yu M, Chen FJ, Arshad M, Xia X, et al. Differential roles of cell death-inducing DNA fragmentation factor-alpha-like effector (CIDE) proteins in promoting lipid droplet fusion and growth in subpopulations of hepatocytes. J Biol Chem 2016;291:4282-4293.
25) Petersen MC, Vatner DF, Shulman GI. Regulation of hepatic glucose metabolism in health and disease. Nat Rev Endocrinol 2017;13:572-587.
26) Hodson L, Skeaff CM, Fielding BA. Fatty acid composition of adipose tissue and blood in humans and its use as a biomarker of dietary intake. Prog Lipid Res 2008;47:348-380.
27) Alkhouri N, Dixon LJ, Feldstein AE. Lipotoxicity in nonalcoholic fatty liver disease: not all lipids are created equal. Expert Rev Gastroenterol Hepatol 2009;3:445-451.
28) Donnelly KL, Smith CI, Schwarzenberg SJ, Jessurun J, Boldt MD, Parks EJ. Sources of fatty acids stored in liver and secreted via lipoproteins in patients with nonalcoholic fatty liver disease. J Clin Invest 2005;115:1343-1343.
29) Tamura S, Shimomura I. Contribution of adipose tissue and de novo lipogenesis to nonalcoholic fatty liver disease. J Clin Invest 2005;115:1139-1142.
30) Lambert JE, Ramos-Roman MA, Browning JD, Parks EJ. Increased de novo lipogenesis is a distinct characteristic of individuals with nonalcoholic fatty liver disease. Gastroenterology 2014;146:726-735.
31) Sunny NE, Parks EJ, Browning JD, Burgess SC. Excessive hepatic mitochondrial TCA cycle and gluconeogenesis in humans with nonalcoholic fatty liver disease. Cell Metab 2011;14:804-810.
32) Drazic A, Myklebust LM, Ree R, Arnesen T. The world of protein acetylation. Biochim Biophys Acta 2016;1864:1372-1401.
33) Anderson KA, Hirschey MD. Mitochondrial protein acetylation regulates metabolism. Essays in Biochemistry 2012;52:23-35.
34) Baeza J, Smallegan MJ, Denu JM. Site-specific reactivity of nonenzymatic lysine acetylation. Acs Chem Biol 2015;10:122-128.
35) Hirschey MD, Shimazu T, Goetzman E, Jing E, Schwer B, Lombard DB, et al. SIRT3 regulates mitochondrial fatty-acid oxidation by reversible enzyme deacetylation. Nature 2010;464:121-125.
36) Laurent G, German NJ, Saha AK, de Boer VC, Davies M, Koves TR, et al. SIRT4 coordinates the balance between lipid synthesis and catabolism by repressing malonyl CoA decarboxylase. Mol Cell 2013;50:686-698.
37) Horton ES. Introduction: an overview of the assessment and regulation of energy balance in humans. Am J Clin Nutr 1983;38:972-977.
38) Poupon V, Begue B, Gagnon J, Dautry-Varsat A, Cerf-Bensussan N, Benmerah A. Molecular cloning and characterization of MT-ACT48, a novel mitochondrial acyl-CoA thioesterase. J Biol Chem 1999;274:19188-19194.
39) Gayral P, Caminade P, Boursot P, Galtier N. The evolutionary fate of recently duplicated retrogenes in mice. J Evol Biol 2007;20:617-626.

Supporting Information

Additional Supporting Information may be found at onlinelibrary.wiley.com/doi/10.1002/hep.31409/suppinfo.